Hindawi Publishing Corporation
EURASIP Journal on Wireless Communications and Networking
Volume 2011, Article ID 980430, 12 pages
doi:10.1155/2011/980430

*Research Article*

# On Channel Estimation for Analog Network Coding in a Frequency-Selective Fading Channel

**Haris Gacanin,[1] Tomas Sjödin,[2] and Fumiyuki Adachi[3]**

[1] *Motive Division, Alcatel-Lucent Bell NV, 2018 Antwerp, Belgium*
[2] *Department of Computing Science, Umeå University, 901 87 Umeå, Sweden*
[3] *Department of Electrical and Communication Engineering, Tohoku University, Sendai 980-8579, Japan*

Correspondence should be addressed to Haris Gacanin, harisg@ieee.org

Received 4 August 2010; Revised 7 November 2010; Accepted 11 January 2011

Academic Editor: Ashish Pandharipande



Recently, broadband analog network coding (ANC) was introduced for high-speed transmission over the wireless (frequency-selective fading) channel. However, ANC requires the knowledge of channel state information (CSI) for self-information removal and coherent signal detection. In ANC, the users' pilot signals interfere during the first slot, which renders the relay unable to estimate CSIs of different users, and, consequently, four time-slot pilot-assisted channel estimation (CE) is required to avoid interference. Naturally, this will reduce the capacity of ANC scheme. In this paper, we theoretically analyze the bit error rate (BER) performance of bi-directional broadband ANC communication based on orthogonal frequency division multiplexing (OFDM) radio access. We also theoretically analyze the performance of the channel estimator's mean square error (MSE). The analysis is based on the assumption of perfect timing and frequency synchronization. The achievable BER performance and the estimator's MSE for broadband ANC is evaluated by numerical and computer simulation. We discuss how, and by how much, the imperfect knowledge of CSI affects the BER performance of broadband ANC. It is shown that the CE scheme achieves a slightly higher BER in comparison with ideal CE case for a low and moderate mobile terminal speed in a frequency-selective fading channel.

## 1. Introduction

Future wireless communication networks are envisaged to provide multimedia broadband services to wireless users. The network capacity must be increased to accommodate these high bandwidth demanding services. Network coding [1] has been used in wired networks to increase the network capacity while its application in wireless relay-assisted networks [2, 3] can exploit the broadcast nature of the wireless medium and further increase the capacity. The relaying can be used to enable bidirectional communication between two users without a direct link between them. The conventional relaying requires four time slots to exchange information between the users, and, consequently, the spectrum efficiency is low.

Network coding at the physical layer (PNC) has been proposed to improve the spectrum efficiency (i.e., doubles the network capacity) of bidirectional relay-assisted communication over the conventional relaying in a flat (i.e., frequency-nonselective) fading channel [4, 5]. Henceforth, we refer to these schemes as narrowband PNC. The scheme enables the users to exchange the information within three time slots in comparison with conventional relaying. Two-slot narrowband analog network coding (ANC) introduced in [6] for bidirectional communication, where the user's signals are mixed in the wireless medium, is an extension of narrowband PNC. Recently [7], broadband ANC based on orthogonal frequency division multiplexing (OFDM) in a frequency-selective fading channel was introduced based on the assumption of perfect knowledge of channel state information (CSI). However, coherent detection and self-information removal in broadband ANC requires accurate amplitude and phase offset estimation (i.e., channel estimation (CE)).

In this paper, we present the performance of bidirectional broadband ANC communication with a pilot-assisted CE

scheme based on OFDM in a frequency-selective fading channel. We theoretically analyze and discuss the performance of broadband ANC with imperfect CSI in terms of the estimator's mean square error (MSE) and bit error rate (BER). The theoretical analysis is based on the assumption that the guard interval (GI) is long enough to avoid the timing problem (i.e., perfect time synchronization) and perfect frequency synchronization. The performance of broadband ANC with imperfect knowledge of CSI is evaluated by Monte Carlo numerical computation method using the derived theoretical expressions and computer simulation. It is shown that the BER performance with imperfect self-information removal for the higher $E_b/N_0$ becomes more sensitive to the estimation errors. The CE error may degrade the BER performances of PNC and ANC differently (since PNC performs digital encoding at the packet level), but in this work, we only consider ANC since it is more spectrum efficient. Moreover, our interest lies on the physical layer techniques design, and the routing problem for ANC is out of the scope of this work.

The reminder of the paper is organized as follows. Section 3 gives an overview of the network model with pilot-assisted CE scheme for ANC in a frequency-selective fading channel. In Section 4, the theoretical BER performance analysis is presented. Numerical results and discussions are presented in Section 5. We summarize our findings in Section 6.

## 2. Related Work

The motivation for ANC is its higher spectrum efficiency in comparison with the conventional relaying and PNC since the bidirectional communication between two users is done via the relay within two time slots. Moreover, ANC has a lower computational complexity since there is no processing at the relay terminal.

The performance of an opportunistic network coding scheme that exploits interference (as in [6]) at the receivers by interpreting it as a form of a network code was investigated in [8]. In [9], the network coding for a multiuser communication problem has been presented and analyzed. The authors in [10] present and analyze an idea to decode the sum of the code-words at the relay followed by a broadcast phase which performs Slepian-Wolf coding with structured codes. The study on wireless multicasting in multiuser network (i.e., two sources to two destinations) with the assistance of a single half-duplex relay was investigated in [11], where the throughput and error performance of different analog and digital relay schemes has been presented. In [12], achievable rates for traditional multihop routing and network coding and various physical-layer network coding (PNC) approaches are considered, and a new method of PNC inspired by Tomlinson-Harashima precoding (THP), where a modulo operation is used to control the power at the relay, was introduced. The outage performance is investigated in [13], where the time-varying nature of the direct link is taken into consideration, and the outage regions of various PNC schemes are theoretically analyzed, and, then, the best combined strategies are derived in terms of the maximum goodput and robustness against the imperfect knowledge of CSI. However, coherent detection and self-information removal in broadband ANC requires accurate amplitude and phase offset estimation (i.e., channel estimation (CE)).

Unlike conventional (without relay) and cooperative (with relay) networks, where signals from different users are separated in time or frequency to avoid interference, in ANC the users' signals interfere in the same time slot. Hence, in the case of pilot transmission, the relay cannot estimate the CSIs of different users. To avoid this problem, a straightforward method is to allocate four time slots for pilot-assisted CE, which reduces the network throughput of ANC scheme. In [14], a complex maximum likelihood (ML) CE for narrowband ANC was presented based on a priori knowledge of the noise variance and the channel cross-correlation coefficients. However, the achievable estimator's MSE is high while the BER performance was not considered at all. Moreover, in [14], a simple symmetric Gaussian channel is assumed. However, in broadband wireless communications networks, the channel frequency selectivity is present due to many propagation paths having different time delays. In [15], the complex maximum likelihood channel estimation is presented for narrowband channels, where the channel gains for the both users are estimated at the relay, and, then, the power allocation algorithm is applied to allocate the power to different channel components so that the detection or CE at the user terminals is optimized. We note that the scheme in [15] requires the knowledge of the noise variance and the channel cross-correlation coefficients of the narrowband channels. In [16], tensor-based CE is presented to obtain the channel gains at both user terminals by solving a complex nonlinear least square problem in an iterative fashion based on a priori known identical and invariant channels over the two time-slots. Note that the design rules in [16] are derived without the effect of noise, which if taken into consideration must be available a priori similar to [14, 15], that may degrade the channel estimator's performance.

For broadband channels, in [17], a two-slot pilot-assisted CE scheme for ANC was presented. In the first slot, both users transmit their pilots to the relay, where one of the pilot signals is cyclically shifted [18] to allow the relay to separate and estimate the CSIs from both users. This stage is named multiple-input single-output channel estimation (MISO-CE) due to its analogy to multiple-input multiple-output (MIMO) OFDM systems [18]. During the second slot, the relay broadcast its pilot signal to the users, which estimate the corresponding CSIs. This stage is named single-input single-output channel estimation (SISO-CE). We note here that only BER performance has been evaluated by computer simulation in [17]. Therefore, in this work, we focus our attention to investigate and analyze the achievable performance of low-complexity pilot-assisted CE for broadband ANC in a frequency-selective fading channel.

## 3. Network Model

Throughout this paper, the following notations are used. Bold lowercase and uppercase letters are used to denote column vectors and matrices, respectively. $(\cdot)^T$, $(\cdot)^*$, $\mathbb{E}[\cdot]$,

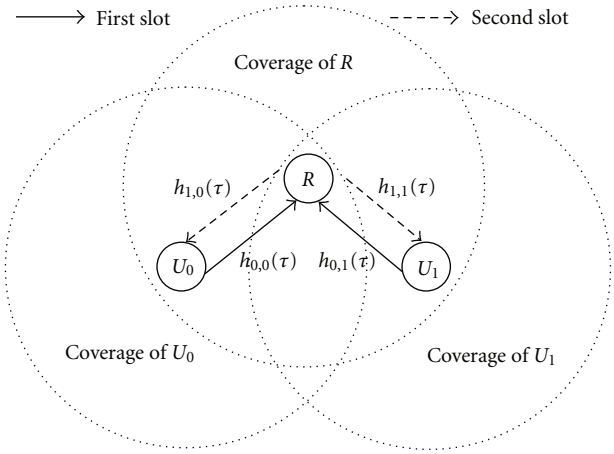


Figure 1: Network model.

$\text{diag}[\cdot]$, $\|\cdot\|$, $\text{Tr}\{\mathbf{A}\}$, and $\|\cdot\|_\infty$ denote transpose, complex conjugate, the ensemble average, diagonal matrix, Euclidean, the trace of the matrix **A,** and maximum norm operations, respectively [19]. A complex Gaussian distribution with mean $\mu$ and variance $\sigma^2$ is denoted by $\mathcal{CN}(\mu, \sigma^2)$. $[\mathbf{a}]_i$ and $[\mathbf{A}]_{ij}$ denote the $i$th element of the vector **a** and element in the $i$th row and $j$th column of **A**, respectively. Finally, **0** and $\mathbf{I}_n$ denote all zero entry and the $n \times n$ identity matrix if otherwise not defined.

*3.1. Transmission Signal Representation.* We consider a two-way relay network with the users, $U_0$ and $U_1$, and the relay $R$ as shown in Figure 1. The users and the relay communicate using time division duplex (TDD) in two slots; (1) $U_0$ and $U_1$ transmit their respective signals to the relay, and (2) the relay broadcasts the received signal to the users using an amplify-and-forward protocol (AF-P).

*First Slot.* The $j$th user $U_j$ data-modulated symbol vector is represented by $\mathbf{d}_j = [d_j(0), d_j(1), \ldots, d_j(N_c-1)]^T$ for $j \in \{0, 1\}$. The $j$th user $U_j$ symbol vector is fed to an $N_c$-point inverse fast Fourier transform (IFFT) to generate the OFDM signal waveform $\mathbf{s}_j = [s_j(0), s_j(1) \ldots s_j(N_c-1)]^T$. An $N_g$-sample guard interval (GI) is inserted, and, then, the signals from the users are transmitted over a frequency-selective fading channel.

The propagation channel can be expressed by the discrete-time channel impulse response given by

$$h_{m,j}(\tau) = \sum_{l=0}^{L-1} h_{l,m,j}\,\delta(\tau - \tau_l), \tag{1}$$

where $L$, $h_{l,m,j}$, $\tau_l$, and $\delta(\tau - \tau_l)$ denote the channel number of paths, the $l$th path gain between the $j$th user $U_j$ and the relay $R$ during the $m$th slot, the $l$th path time delay normalized by the sampling period of IFFT (i.e., $T_c$), and the delta function, respectively.

The signal received at the relay, $\mathbf{r}_r = [r_r(0), r_r(1) \ldots r_r(N_c-1)]^T$, can be expressed in the frequency domain as

$$\mathbf{r}_r = \sqrt{S}\sum_{j=0}^{1} \mathbf{H}_{0,j}\mathbf{d}_j + \mathbf{n}_r, \tag{2}$$

where $S(= E_s/T_c)$, $\mathbf{H}_{m,j} = \text{diag}[H_{m,j}(0), H_{m,j}(1), \ldots, H_{m,j}(N_c-1)]$ and $\mathbf{n}_r = [n_r(0), n_r(1), \ldots, n_r(N_c-1)]^T$, respectively, denote the transmit signal power, the channel gain matrix between the $j$ user $U_j$ and the relay $R$ at the $m$th slot with $H_{m,j}(n) = \text{FFT}\{h_{m,j}(\tau)\}$ and the noise vector which elements are modeled as $\mathcal{CN}(0, \sigma_n^2)$ with $\sigma_n^2 = N_0/T_c$. $E_s$ and $N_0$ denote the data-modulated symbol energy and the single-sided noise power spectral density. Note that the frequency domain signal representation at the relay is used for the sake of consistency with the following analysis.

*Second Slot.* The relay amplifies the received signal by $\sqrt{S}$ and broadcasts $\widetilde{\mathbf{r}}_r = \sqrt{S}\mathbf{r}_r$. After GI removal and $N_c$-point FFT, the signal received at the $j$th user $U_j$ can be expressed as

$$\mathbf{r}_j = \mathbf{H}_{1,j}\widetilde{\mathbf{r}}_r + \mathbf{n}_j. \tag{3}$$

The $j$th user $U_j$ first removes its self-information as

$$\widetilde{\mathbf{r}}_j = \mathbf{r}_j - \mathbf{H}_{1,j}\mathbf{H}_{0,j}\mathbf{d}_j, \tag{4}$$

where $\mathbf{d}_j$ denotes the $j$th user $U_j$s data-modulated self-information vector. Then, one-tap zero forcing frequency domain equalization (ZF-FDE) is applied as

$$\widehat{\mathbf{r}}_j = \mathbf{W}_j\widetilde{\mathbf{r}}_j. \tag{5}$$

The $j$th user $U_j$ equalization weight matrix $\mathbf{W}_j$ is chosen to satisfy the condition $\mathbf{H}_{1,j}\mathbf{H}_{0,\bar{j}}\mathbf{W}_j = \mathbf{I}_{N_c}$ and it is given by

$$\mathbf{W}_j = \text{diag}\left[\frac{1}{H_{0,\bar{j}}(0)H_{1,j}(0)}, \frac{1}{H_{0,\bar{j}}(1)H_{1,j}(1)}, \ldots, \frac{1}{H_{0,\bar{j}}(N_c-1)H_{1,j}(N_c-1)}\right], \tag{6}$$

where the bar over $j$ signifies the unitary complement operation (i.e., "NOT" operation) that performs logical negation of $j$.

Estimates of the channel gains are required to perform self-information removal and equalization given by (4) and (5), respectively. The channel gain matrix $\mathbf{H}_{m,j}$ is replaced in (4) and (5) by the channel gain estimate matrix $\mathbf{H}^e_{m,j}$ for $m, j \in \{0, 1\}$.

*3.2. Channel Estimation [17].* This section is devoted, in part, to the problem statement of conventional CE for ANC scheme, and, then, the proposed pilot-assisted CE scheme and its MSE performance analysis are presented.

*3.2.1. Problem Statement.* If a classical CE approach is to be used with ANC scheme the following problems arise.

(i) In both conventional (without relaying) and cooperative (relay-assisted) networks, different users' pilot signals are separated by orthogonal frequencies or different time slots to avoid interference as shown in [20, 21]. However, in ANC, the users transmit simultaneously during the first time slot, and, as a result of this, the pilot signals interfere with each other. Consequently, the relay cannot estimate the CSIs of different users.

(ii) To estimate all CSIs in bidirectional ANC scheme, a conventional method is to allocate four time slots to separate different users' pilot signals. However, this significantly reduces the network throughput since additional two slots must be added for pilot-assisted CE.

(iii) The channels between the users and the relay are estimated at the relay during the first slot. These estimated CSIs have to be fed back to the user terminals, which additionally reduces the throughput. The problem of CSI feedback is not considered in this work, and it is left as an interesting future work. We note that we theoretically analyze the channel estimator's performance in terms of MSE and BER (see Sections 4.1 and 4), and, thus, the assumption of an ideal feedback channel simplifies the analysis (if a nonideal feedback channel is assumed, the theoretical analysis may become very difficult if not impossible).

To address the above-mentioned problems (1) and (2) the proposed CE is presented below.

*3.2.2. Two-Slot CE for Broadband ANC [17].* Unlike the conventional approach, where four time slots must be allocated to support bidirectional communication, we present a two-slot pilot-assisted CE scheme for bidirectional ANC with two users assisted by a relay.

The channel estimation scheme for broadband ANC network is illustrated in Figure 2. The figure shows that ANC scheme can be seen as a multiple-input single-output (MISO) system during the first slot and two independent single-input single-output (SISO) systems during the second slot. Consequently, the first slot of the CE process, illustrated in Figure 2(a), is based on the MISO-CE principle since the signals from two users' antennas are received by a single antenna at the relay. The second slot of the CE process, illustrated in Figure 2(b), is based on two independent SISO-CE schemes. It is assumed that the users are out of each others coverage area, and, consequently, the signals received by each user's antenna are independent. Thus, we refer to the second CE stage as SISO-CE rather than a single-input multiple-output- (SIMO-) CE. Note that in the first CE stage, both user signals arrive at the relay's antenna at the same time, and, thus, we refer to this stage as MISO-CE.

Figure 3 illustrates the pilot and data transmission frame structure of the two users, $U_0$ and $U_1$, and the relay $R$. The pilot and data frames are divided in two time slots, where each slot has a length of $N_c + N_g$ samples, where $N_c$ and $N_g$, respectively, denote the number of subcarriers and the GI length. The first slot of the pilot frame corresponds to the MISO-CE, which is used to transmit the pilot signals, $p_0(t)$ and $p_1(t)$, from $U_0$ and $U_1$, respectively, as illustrated in Figure 2(a). The second slot is used by the relay during the SISO-CE to broadcast its pilot signal $p_0(t)$ to the users as illustrated in Figure 2(b). The pilot frame transmission is followed by $N_b$ data frames as shown in Figure 3.

*MISO-CE.* The users, $U_0$ and $U_1$, transmit their pilots to the relay $R$ over a frequency-selective fading channel during the first slot of a pilot frame as shown in Figure 3.

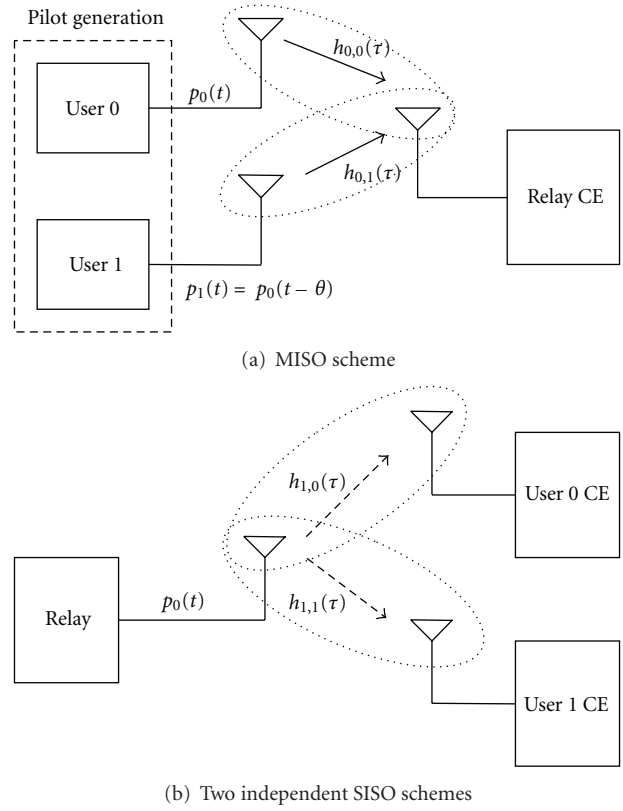


Figure 2: Proposed CE scheme.

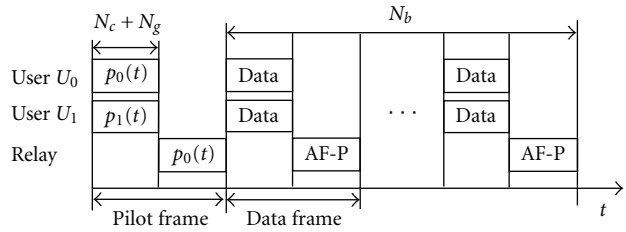


Figure 3: Pilot and data transmission frame.

After GI removal and $N_c$-point FFT, the pilot signal received at the relay $R$ can be represented as

$$\mathbf{r}_{r,p} = \sqrt{S}\sum_{j=0}^{1}\mathbf{H}_{0,j}\mathbf{P}_j + \mathbf{n}_r, \tag{7}$$

where $\mathbf{P}_j = \text{diag}[P_j(0), P_j(1), \ldots, P_j(N_c-1)]$ with $P_j(n) = \text{FFT}\{p_j(t)\}$. To avoid overlapping of the CSIs from different users during the first slot, the pilot signal $\{p_1(t)\}$ of $U_1$ is cyclicly shifted by $\theta$ samples relative to the pilot signal $\{p_0(t)\}$ of $U_0$; $\{p_1(t) = p_0((t-\theta) \bmod N_c); t = 0 \sim N_c - 1\}$ as used in MIMO-OFDM systems [18].

Using the time-shifting property of Fourier transform applied to $\{p_1(t) = p_0((t-\theta) \bmod N_c); t = 0 \sim N_c - 1\}$ [22] in (7) we obtain

$$\mathbf{r}_{r,p}(n) = \sqrt{S}\mathbf{H}_{0,0}\mathbf{P}_0 + \sqrt{S}\mathbf{H}_{0,1}\mathbf{\Theta}_f\mathbf{P}_0 + \mathbf{n}_r, \tag{8}$$

where $\mathbf{\Theta}_f = \text{diag}[1, \exp(-j2\pi(\theta/N_c)), \ldots, \exp(-j2\pi(N_c-1)(\theta/N_c))]$. To avoid overlapping of different users CSIs the time shift $\theta$ is chosen to be larger than the GI length since we assume that the channel number of paths $L$ does not exceeds the GI. The estimate of the channel gain is obtained by reverse modulation as

$$\mathbf{H}_{r,e} = \mathbf{r}_{r,p}\mathbf{P}_0^{-1} = \sqrt{S}\mathbf{H}_{0,0} + \sqrt{S}\mathbf{H}_{0,1}\mathbf{\Theta}_f + \tilde{\mathbf{n}}_r, \tag{9}$$

where $\tilde{\mathbf{n}}_r = \mathbf{n}_r\mathbf{P}_0^{-1}$. Then, $N_c$-point IFFT is applied to transform the estimated channel gain into the estimated CSI vector, $\mathbf{h}_{r,e} = [h_{r,e}(0), \ldots, h_{r,e}(\tau), \ldots, h_{r,e}(N_c-1)]^T$, given by

$$\mathbf{h}_{r,e} = \mathbf{F}^H\mathbf{H}_{r,e} = \sqrt{S}\mathbf{h}_{0,0} + \sqrt{S}\overline{\mathbf{h}}_{0,1} + \mathbf{F}^H\tilde{\mathbf{n}}_r, \tag{10}$$

where $\mathbf{F}$ and $\overline{\mathbf{h}}_{0,1}$, respectively, denote the FFT matrix [19] and the time domain shifted CSI vector of $\mathbf{h}_{0,1}$. The estimated CSI vector $\mathbf{h}_{r,e}$ is illustrated in Figure 4(a). A filter $\mathbf{Q}_{N_c}^j$ is used to separate the $j$th user's ($U_j$'s) estimated CSI vector, $\mathbf{h}_{0,j}^e = [h_{0,j}^e(0), \ldots, h_{0,j}^e(\tau), \ldots, h_{0,j}^e(N_c-1)]^T$, during the first slot represented as

$$\mathbf{h}_{0,j}^e = \mathbf{Q}_{N_c}^j\mathbf{h}_{r,e}, \tag{11}$$

with

$$\mathbf{Q}_{N_c}^0 = \begin{pmatrix} \mathbf{I}_{N_g} \\ \mathbf{0}_{N_c-N_g\times N_c} \end{pmatrix}$$
$$\mathbf{Q}_{N_c}^1 = \begin{pmatrix} \mathbf{A}_{\theta\times N_c} \\ \mathbf{B}_{(N_c-\theta)\times N_c} \end{pmatrix}\begin{pmatrix} \mathbf{0}_{\theta\times N_c} \\ \mathbf{C}_{N_g\times N_c} \\ \mathbf{0}_{(N_c-N_g-\theta)\times N_c} \end{pmatrix}, \tag{12}$$

where $\mathbf{0}$, $\mathbf{A}$, $\mathbf{B}$, and $\mathbf{C}$, respectively, denote all zero entry, the matrix represented by the rows from $\theta$ until $\theta + N_g$ of $\mathbf{I}_{N_c}$, the matrix represented by the last $N_c - \theta$ rows of $\mathbf{I}_{N_c}$, and the matrix represented by the first $N_g$ rows of $\mathbf{I}_{N_c}$. The $j$th user $U_j$ filtered CSI vector estimate $\mathbf{h}_{0,j}^e = [h_{0,j}^e(0), \ldots, h_{0,j}^e(\tau)\ldots, h_{0,j}^e(N_c-1)]^T$ for $j \in \{0,1\}$ is illustrated in Figures 4(b) and 4(c), respectively. After filtering, the estimated CSI vector $\mathbf{h}_{0,1}$ is shifted by $\theta$ samples as shown in Figure 4(c).

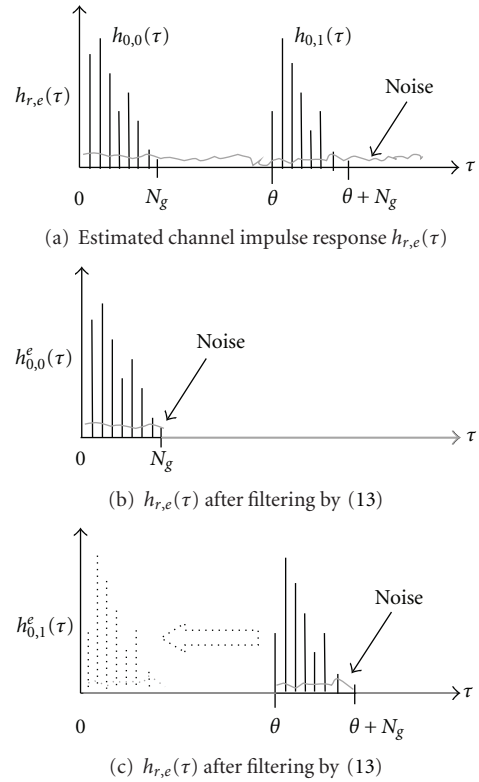


(a) Estimated channel impulse response $h_{r,e}(\tau)$

(b) $h_{r,e}(\tau)$ after filtering by (13)

(c) $h_{r,e}(\tau)$ after filtering by (13)

FIGURE 4: Estimation of the channel impulse responses ($h_{0,0}^e$ and $h_{0,1}^e$ between the relay and the first and second user during the first transmission stage).

Finally, an $N_c$-point FFT is applied to $\mathbf{h}_{0,j}^e$ to obtain the estimate of the channel gain $\mathbf{H}_{0,j}^e$ between the relay $R$ and the $j$th user $U_j$ during the first slot given by

$$\mathbf{H}_{0,j}^e = \mathbf{F}\mathbf{Q}_{N_c}^j\mathbf{F}^H\mathbf{H}_{r,e} = \sqrt{S}\mathbf{H}_{0,j} + \mathbf{F}\mathbf{Q}_{N_c}^j\mathbf{F}^H\tilde{\mathbf{n}}_r. \tag{13}$$

Note that (13) holds as long as $\theta$ is chosen to be larger than the channel number of paths $L$.

*SISO-CE.* The relay $R$ broadcasts its pilot sequence, $p_0(t)$, to both users, $U_0$ and $U_1$, during the second slot of the pilot frame as shown in Figure 3. Without loss of generality, we focus on the processing of the $j$th user $U_j$ for $j \in \{0,1\}$ as presented below.

The pilot signal received at the $j$th user $U_j$ can be expressed as

$$\mathbf{r}_{j,p} = \sqrt{S}\mathbf{H}_{1,j}\mathbf{P}_0 + \mathbf{n}_j. \tag{14}$$

The estimate of the channel gain matrix $\mathbf{H}_{1,j}^e$ is obtained as [20]

$$\mathbf{H}_{j,e} = \mathbf{r}_{j,p}\mathbf{P}_0^{-1} = \sqrt{S}\mathbf{H}_{1,j} + \tilde{\mathbf{n}}_j, \tag{15}$$

where $j \in \{0,1\}$ and $\tilde{\mathbf{n}}_j(n) = \mathbf{n}_j\mathbf{P}_0^{-1}$. Then, $N_c$-point IFFT is applied to $\mathbf{H}_{j,e}$, to obtain the estimated CSI

vector $\mathbf{h}_{j,e}$ between the relay $R$ and the $j$th user $U_j$. The estimated CSI vector is filtered by $\mathbf{Q}_{N_c}^0$ for $j \in \{0,1\}$ as $\mathbf{h}_{1,j}^e = \mathbf{Q}_{N_c}^0 \mathbf{h}_{j,e}$. Finally, the filtered signal is fed to $N_c$-point FFT to obtain the channel gain matrix estimate $\mathbf{H}_{1,j}^e = \text{diag}[H_{1,j}^e(0), H_{1,j}^e(1), \ldots, H_{1,j}^e(N_c - 1)]$ between the relay $R$ and the $j$th user $U_j$ during the second slot.

The estimates of CSI during the MISO-CE stage are required at the users terminals. In this paper, we assume that the channel gains, $\mathbf{H}_{0,j}^e$ for $j \in \{0,1\}$, are sent from the relay to the users by an ideal feedback channel. The channel gain matrix $\{H_{m,j}^e(n)\}$ for $m, j \in \{0,1\}$ is used by the users $U_0$ and $U_1$ to remove self-information and detect the signal from the partner as described in Section 3.

## 4. Performance Analysis

This section is devoted to theoretical analysis of broadband ANC with imperfect knowledge of CSI. We first derive the channel estimators MSE, and, then, the expressions for decision variables with the conditional BER expressions are presented. Note that the analysis is based on the assumption of perfect timing and frequency synchronization, and their impacts on the performance of bidirectional broadband ANC are left as an interesting future work.

*4.1. Channel Estimator's MSE.* Here, we evaluate the MSE of the CE scheme. For convenience, we assume that the propagation channels between the users and relay $R$ have the equal number of paths $L$. The MSE of the estimated channel gain $\mathbf{H}_{m,j}^e$ during the $m$th slot is defined by

$$\text{MSE}_m = \mathbb{E}\left[\left|\left|\mathbf{H}_{m,j}^e - \mathbf{H}_{m,j}\right|\right|^2\right], \tag{16}$$

where $\mathbf{H}_{m,j}^e$ denotes the estimated channel matrix between the relay $R$ and the $j$th user at the $m$th slot.

*MIMO-CE.* The channel gain estimate $\mathbf{H}_{0,j}^e$ is an unbiased estimation of $\mathbf{H}_{0,j}$ since $\mathbb{E}[\mathbf{H}_{0,j}^e] = \mathbf{H}_{0,j}$. Using (13) and (16), the MSE of the estimated channel gain $\mathbf{H}_{0,j}^e$ for $j \in \{0,1\}$ during the first slot is given by

$$\text{MSE}_0 = \mathbb{E}\left[\left|\left|\mathbf{F}\mathbf{Q}_{N_c}^j \mathbf{F}^H \tilde{\mathbf{n}}_r\right|\right|^2\right] = \frac{\sigma_n^2}{N_c}\text{Tr}\left\{\mathbf{T}\mathbf{T}^H\right\} = \frac{N_g}{N_c}\sigma_n^2, \tag{17}$$

where we assumed $\mathbf{P}_0^H \mathbf{P}_0 = \mathbf{I}_{N_c}$ and $\mathbf{T} = \mathbf{F}_{N_g}$. Although different CE schemes (i.e., MISO-CE and SISO-CE) are applied for different users, the MSE is not a function of the user parameter $j$ as shown by (17).

*SISO-CE.* The channel gain estimate $\mathbf{H}_{1,j}^e$ is an unbiased estimation of $\mathbf{H}_{1,j}$ since $\mathbb{E}[\mathbf{H}_{1,j}^e] = \mathbf{H}_{1,j}$. Using (15) and (16), the MSE of the estimated channel gain $\mathbf{H}_{1,j}^e$ for $j \in \{0,1\}$ during the second slot is given by

$$\text{MSE}_1 = \mathbb{E}\left[\left|\left|\mathbf{F}\mathbf{Q}_{N_c}^0 \mathbf{F}^H \tilde{\mathbf{n}}_r\right|\right|^2\right] = \frac{\sigma_n^2}{N_c}\text{Tr}\left\{\mathbf{T}\mathbf{T}^H\right\} = \frac{N_g}{N_c}\sigma_n^2. \tag{18}$$

This confirms that the MSE of the channel estimator for MISO-CE and SISO-CE are the same. Finally, the average MSE is given by $\text{MSE} = 1/2 \sum_{m=0}^{1} \text{MSE}_m$.

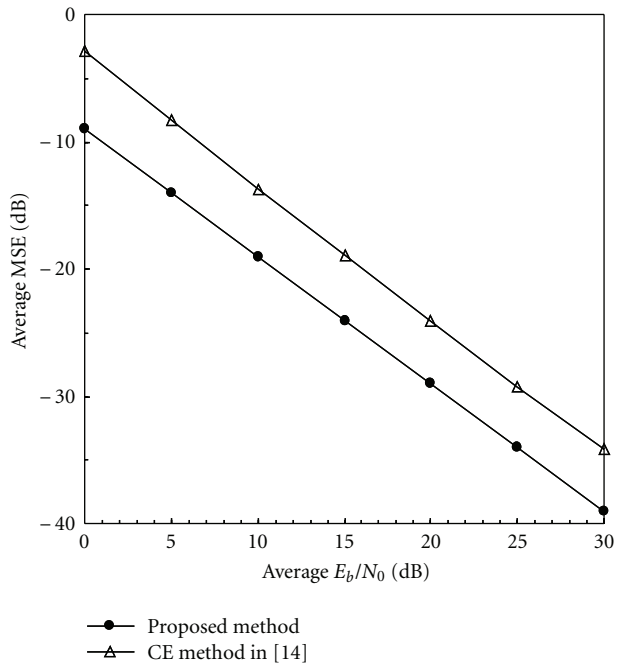


Figure 5: Average MSE versus $E_b/N_0$.

The theoretical average MSE of the proposed CE scheme and the estimator presented in [14] are illustrated in Figure 5. It can be seen from the figure that the proposed channel estimator achieves a lower MSE in comparison with the estimator in [14].

*4.2. Decision Variables.* We begin by developing a general mathematical model for decision variables in three cases; (1) effect of imperfect knowledge of CSI, (2) effect of self-information removal due to imperfect knowledge of CSI, and (3) perfect knowledge of CSI and self-information removal. We note here that imperfect self-information removal may be caused by different factors such as imperfect synchronization, carrier frequency offset, imperfect knowledge of CSI, and so forth. In this paper, we only consider the impact of imperfect knowledge of CSI on the self-information removal.

For the sake of brevity, we focus only on the $j$th user $U_j$ and define diagonal matrix $\mathbf{H}_j = \mathbf{H}_{0,\bar{j}}\mathbf{H}_{1,j}$. We assume that channel estimation error of the $j$th user $U_j$ can be modeled as

$$\mathbf{H}_j^e = \mathbf{H}_j + \mathbf{E}_j, \tag{19}$$

where $\mathbf{E}_j = \text{diag}[E_j(0), E_j(1), \ldots, E_j(N_c - 1)]$ denote the the channel estimation error matrix of the $j$th user $U_j$. It is assumed that elements of $\mathbf{E}_j$ are modeled as $\mathcal{CN}(0, \sigma_e^2)$, where elements of $\mathbf{E}_j$ and $\mathbf{H}_j$ are statistically independent.

*4.2.1. Effect of Imperfect Knowledge of CSI.* Substituting (3), (4), and (19) into (5), the decision variable with imperfect knowledge of CSI can be represented as

$$\hat{\mathbf{d}}_j = \left(\mathbf{H}_j^{eH}\mathbf{H}_j^{e}\right)^{-1}\mathbf{H}_j^{eH}\mathbf{H}_j\mathbf{d}_{\overline{j}} - \left(\mathbf{H}_j^{eH}\mathbf{H}_j^{e}\right)^{-1}\mathbf{H}_j^{eH}\mathbf{E}_{\overline{j}}\mathbf{d}_j + \left(\mathbf{H}_j^{eH}\mathbf{H}_j^{e}\right)^{-1}\mathbf{H}_j^{eH}\left(\mathbf{H}_{1,j}\mathbf{n}_r + \mathbf{n}_j\right), \tag{20}$$

where $\mathbf{E}_{\overline{j}}$ denotes the channel estimation error matrix of $\mathbf{H}_{1,j}\mathbf{H}_{0,j}$.

Using (19) and the Sherman-Morisson formula [19], (20) can be rewritten as

$$\hat{\mathbf{d}}_j = \mathbf{d}_{\overline{j}} - \left(\mathbf{H}_j + \mathbf{E}_j\right)^{-1}\mathbf{E}_j\mathbf{d}_{\overline{j}} - \left(\mathbf{I}_{N_c} - \left(\mathbf{H}_j + \mathbf{E}_j\right)^{-1}\mathbf{E}_j\right)\mathbf{E}_{\overline{j}}\mathbf{d}_j + \left(\mathbf{H}_j + \mathbf{E}_j\right)^{-1}\left(\mathbf{H}_{1,j}\mathbf{n}_r + \mathbf{n}_j\right), \tag{21}$$

where the first term denotes the desired signal; the second term denotes the effect of imperfect knowledge of CSI on the desired signal; the third term denotes the interference due to imperfect self-information removal; the last term denotes the noise. Next, we derive the signal and interference powers due to channel estimation errors.

The signal power is given by

$$\mathbf{P}_{j,\mathrm{I}} = \mathbb{E}\left[\left|\left[\mathbf{d}_{\overline{j}}\right]_i\right|^2\right] = \frac{E_s}{T_c}. \tag{22}$$

The interference power of the desired signal due to imperfect knowledge of CSI is given by (Appendix A)

$$\mathbf{P}_{j,\mathrm{II}} = \mathbb{E}\left[\left|\left[\left(\mathbf{H}_j + \mathbf{E}_j\right)^{-1}\mathbf{E}_j\mathbf{d}_{\overline{j}}\right]_i\right|^2\right] \approx \frac{E_s}{T_c}\widetilde{\mathbf{P}}_{j,\mathrm{II}}, \tag{23}$$

where

$$\widetilde{\mathbf{P}}_{j,\mathrm{II}} = 2\sigma_e^2\,\mathrm{diag}\left[\frac{\Delta(0)}{\left|H_j(0)\right|^2}, \frac{\Delta(1)}{\left|H_j(1)\right|^2}, \ldots, \frac{\Delta(N_c-1)}{\left|H_j(N_c-1)\right|^2}\right] \tag{24}$$

and $\Delta(n) = 1 + 3(2\sigma_e^2/|H_j(n)|^2) + 5(2\sigma_e^2/|H_j(n)|^2)^2$. The interference power due to imperfect self-information removal is given by (Appendix B)

$$\mathbf{P}_{j,\mathrm{III}} = \mathbb{E}\left[\left|\left[\left(\mathbf{I}_{N_c} - \left(\mathbf{H}_j + \mathbf{E}_j\right)^{-1}\mathbf{E}_j\right)\mathbf{E}_{\overline{j}}\mathbf{d}_j\right]_i\right|^2\right] \approx \frac{E_s}{T_c}2\sigma_e^2\left(\mathbf{I}_{N_c} + \widetilde{\mathbf{P}}_{j,\mathrm{II}}\right). \tag{25}$$

Finally, the noise power is given by (Appendix C)

$$\mathbf{P}_{j,\mathrm{IV}} = \mathbb{E}\left[\left|\left[\left(\mathbf{H}_j + \mathbf{E}_j\right)^{-1}\left(\mathbf{H}_{1,j}\mathbf{n}_r + \mathbf{n}_j\right)\right]_i\right|^2\right] = \frac{N_0}{T_c}\widetilde{\mathbf{P}}_{j,\mathrm{IV}}\left(\mathbf{I}_{N_c} + \widetilde{\widetilde{\mathbf{P}}}_{j,\mathrm{IV}}\widetilde{\mathbf{P}}_{j,\mathrm{II}}\right) + \frac{N_0}{T_c}\widetilde{\widetilde{\mathbf{P}}}_{j,\mathrm{IV}}\left(\mathbf{I}_{N_c} + \widetilde{\mathbf{P}}_{j,\mathrm{II}}\right), \tag{26}$$

where

$$\widetilde{\mathbf{P}}_{j,\mathrm{IV}} = \mathrm{diag}\left[\left|H_{1,j}(0)\right|^2, \left|H_{1,j}(1)\right|^2, \ldots, \left|H_{1,j}(N_c-1)\right|^2\right],$$

$$\widetilde{\widetilde{\mathbf{P}}}_{j,\mathrm{IV}} = \mathrm{diag}\left[\frac{1}{\left|H_j(0)\right|^2}, \frac{1}{\left|H_j(1)\right|^2}, \ldots, \frac{1}{\left|H_j(N_c-1)\right|^2}\right]. \tag{27}$$

Next, we present the decision variables in the case of imperfect self-information removal due to imperfect knowledge of CSI at the relay and destination terminals.

*4.2.2. Effect of Self-Information Removal due to Imperfect Knowledge of CSI.* Here, we only consider the effect of imperfect self-information removal resulting from imperfect knowledge of CSIs. Thus, (21) can be rewritten as

$$\hat{\mathbf{d}}_j = \mathbf{d}_{\overline{j}} - \left(\mathbf{I}_{N_c} - \left(\mathbf{H}_j + \mathbf{E}_j\right)^{-1}\mathbf{E}_j\right)\mathbf{E}_{\overline{j}}\mathbf{d}_j + \mathbf{H}_j^{-1}\left(\mathbf{H}_{1,j}\mathbf{n}_r + \mathbf{n}_j\right), \tag{28}$$

where the first denotes the desired signal power given by (22); the second term denotes the interference power due to imperfect self-information removal given by (25); the third term denotes the noise power given by

$$\mathbf{P}_{j,\mathrm{IV}} = \mathbb{E}\left[\left|\left[\mathbf{H}_j^{-1}\left(\mathbf{H}_{1,j}\mathbf{n}_r + \mathbf{n}_j\right)\right]_i\right|^2\right] = \frac{N_0}{T_c}\,\mathrm{diag}\left[\frac{\left|H_{1,j}(0)\right|^2 + 1}{\left|H_j(0)\right|^2}, \frac{\left|H_{1,j}(1)\right|^2 + 1}{\left|H_j(1)\right|^2}, \ldots, \frac{\left|H_{1,j}(N_c-1)\right|^2 + 1}{\left|H_j(N_c-1)\right|^2}\right]. \tag{29}$$

Note that in this case $\mathbf{P}_{j,\mathrm{II}} = 0$. Next, we present the decision variables in the case of perfect knowledge of CSI at the relay and destination terminals.

*4.2.3. Perfect Knowledge of CSI.* In this case, the channel estimation error $\mathbf{E}_j = \mathrm{diag}[\mathbf{0}]$ and (21) can be rewritten as

$$\hat{\mathbf{d}}_j = \mathbf{d}_{\overline{j}} + \mathbf{H}_j^{-1}\left(\mathbf{H}_{1,j}\mathbf{n}_r + \mathbf{n}_j\right), \tag{30}$$

where the first and second terms denote the desired signal and the noise, respectively. The desired signal power $\mathbf{P}_{j,\mathrm{I}}$ is given by (22) while the noise power is given by (29). Note that in this case $\mathbf{P}_{j,\mathrm{II}} = \mathbf{P}_{j,\mathrm{III}} = \mathbf{0}$.

*4.3. BER.* We assume all "1" transmission without loss of generality and quaternary phase shift keying (QPSK) data-modulation (i.e., $d_j(n) = (1 + \jmath)/\sqrt{2}$, where $\jmath$ denotes the complex operator). The $j$th user $U_j$ instantaneous signal-to-interference plus noise ratio (SINR) $\gamma_j(i)$ of the $i$th symbol in the transmitted data vector $\mathbf{d}_{\overline{j}}$ is given as

$$\gamma_j\left(\frac{E_s}{N_0}, \mathbf{H}_{m,j}, i\right) = \frac{[\mathbf{P}_{\mathrm{I}}]_{ii}}{\left[\mathbf{P}_{j,\mathrm{II}}\right]_{ii} + \left[\mathbf{P}_{j,\mathrm{III}}\right]_{ii} + \left[\mathbf{P}_{j,\mathrm{IV}}\right]_{ii}}. \tag{31}$$

The conditional BER of the $i$th data symbol for the given $\mathbf{H}_{m,j}$ is given by

$$P_{j,b}\left(\frac{E_s}{N_0}, \mathbf{H}_{m,j}, i\right) = \frac{1}{2}\,\mathrm{erfc}\left(\sqrt{\frac{\gamma_j\left(E_s/N_0, \mathbf{H}_{m,j}, i\right)}{2}}\right), \quad (32)$$

where $\mathrm{Erfc}(\cdot)$ is the complementary error function [22]. The theoretical average BER of the $\overline{j}$th user $U_{\overline{j}}$ transmitted data vector $\mathbf{d}_j$ is numerically evaluated by averaging (32) over all possible realizations of $\mathbf{H}_{m,j}$ for all $i$ as

$$P_{j,b}\left(\frac{E_s}{N_0}\right) = \frac{1}{N_c}\sum_{i=0}^{N_c-1}\mathbb{E}\left[P_{j,b}\left(\frac{E_s}{N_0}, \mathbf{H}_{m,j}, i\right)\right]. \quad (33)$$

The evaluation of the theoretical average BER is done by Monte-Carlo numerical computation method based on the analysis presented in Section 4 as follows. A set of path gains $\{h_{m,l}; l = 0 \sim L-1\}$ is generated using (1) to obtain the channel gain matrix $\mathbf{H}_{m,j}$ for $j \in \{0, 1\}$, and, then, the equalization matrix $\mathbf{W}_j$ is computed using (6) for each source terminal. The conditional BER as a function of the average signal energy per symbol-to-AWGN power spectrum density ratio $E_s/N_0$ is computed using (32) for the given set of path gains $\{h_{m,l}; l = 0 \sim L-1\}$. This is repeated a sufficient number of times to obtain the theoretical average BER given by (33).

## 5. Numerical Results and Discussions

The parameters used for numerical evaluation are summarized in Table 1. We assume the OFDM system with $N_c = 256$-subcarriers, $N_g = 32$ and ideal coherent QPSK modulation and demodulation with $E[|d_j(n)|^2] = 1$. The propagation channel is $L = 16$-path block Rayleigh fading channel, where $\{h_{l,m,j}; l = 0 \sim L-1\}$ are zero-mean independent complex variables with $E[|h_{l,m,j}|^2] = 1/L$. We assume $\tau_0 = 0 < \tau_1 < \cdots < \tau_{L-1}$ and that the $l$th path time delay is $\tau_l = l\Delta$, where $\Delta(\geq 1)$ is the time delay separation between the previous and following path. The maximum channel time delay is less than the GI length, and all channel paths are independent of each other. $f_D T_s$ represents the normalized Doppler frequency, where $1/T_s = 1/[T_c(1 + (N_g/N_c))]$ is the transmission symbol rate ($f_d T_s = 10^{-4}$ corresponds to a mobile terminal speed of approximately 19 km/h for a transmission data rate of 100 Msymbols/s and a carrier frequency of 2 GHz). We assume error-free feedback channel from the relay $R$ to the users and no shadowing nor path loss. As a pilot, we use a Chu-sequence given by $\{p_0(t) = \exp\{j\pi t^2/N_c\}; t = 0 \sim N_c - 1\}$ [23]. In this work, we assume that the GI is long enough to avoid the timing problem (i.e., perfect time synchronization) and perfect frequency synchronization.

*5.1. Effect of Imperfect Knowledge of CSI and Self-Information Removal.* First, we discuss the overall impact of channel estimation error $\sigma_e^2$ on the achievable BER performance. Later we investigate the effect of self-information removal, when the effect of imperfect CSI on the desired signal is not taken into consideration.

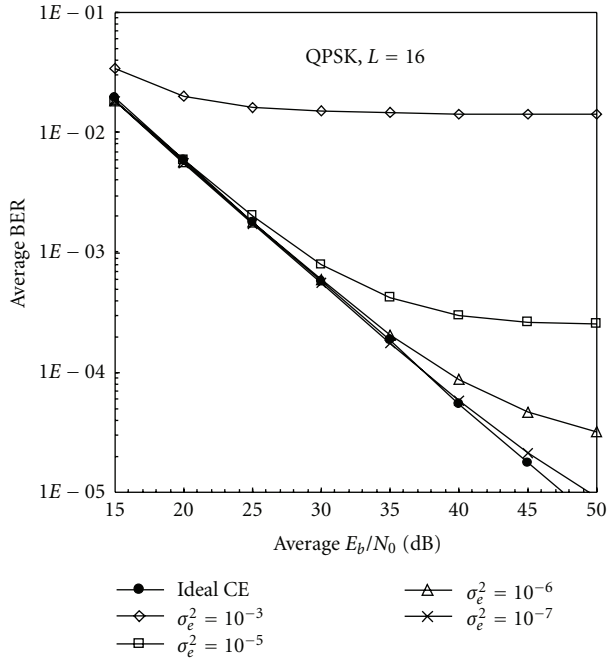


Figure 6: Impact of $\sigma_e^2$ on average BER.

Figure 6 illustrates the BER performance as a function of the average signal energy per bit-to-AWGN power spectrum density ratio $E_b/N_0 (= 0.5 \times (E_s/N_0) \times (1 + (N_g/N_c)))$ with the channel estimation error variance $\sigma_e^2$ as a parameter. The figure shows that the BER performance of broadband ANC scheme degrades as the channel estimation error variance $\sigma_e^2$ increases from $10^{-7}$. On the other hand, to evaluate the impact of self-information removal due to imperfect knowledge of CSI, we plot the BER performance as a function of the channel estimation error variance $\sigma_e^2$ is illustrated in Figure 7.

The figure illustrates the achievable BER performance as a function of the channel estimation error variance $\sigma_e^2$ with $E_b/N_0$ as a parameter. The terms "Perfect CSI", "Effect of S-IR", and "Effect of CE" in Figure 7, respectively, denote the BER performance with perfect knowledge of CSI at all terminals given by (30), the effect of self-information removal due to imperfect knowledge of CSI given by (28) and the overall performance degradation due to imperfect knowledge of CSI given by (21). The figure shows that the BER performance with imperfect knowledge of CSI at the destination and relay terminals is sensitive on the channel estimation error variance $\sigma_e^2$ depending on the level of $E_b/N_0$; for higher value of $E_b/N_0$, the system becomes more sensitive to the channel estimation error. The figure confirms that the BER performance with imperfect self-information removal for the higher $E_b/N_0$ becomes more sensitive to the CE error. This is because the small value of $\sigma_e^2$ during the self-information removal still keeps a large portion of the desired

Table 1: Simulation parameters.

| | | |
|---|---|---|
| Transmitter $(U_0, U_1)$ | Block size | $N_c = 256$ |
| | GI | $N_g = 32$ |
| | Data modulation | QPSK |
| Channel | $L$-path block Rayleigh fading with $\Delta = 1$ | |
| Relay | Protocol | Amplify-and-forward |
| | Feedback | Perfect |
| Receiver $(U_0, U_1)$ | FDE | ZF |
| | Channel estimation | Pilot-assisted |

signal at a high $E_b/N_0$ level, which significantly affects the BER performance.

*5.2. BER Performance.* Figure 8 illustrates the BER performance as a function of the average signal energy per bit-to-AWGN power spectrum density ratio $E_b/N_0 (= 0.5 \times (E_s/N_0) \times (1 + (N_g/N_c)) \times (1 + (1/N_b)))$ with the number of data frames $N_b$ as a parameter. The power loss due to GI and pilot insertion is taken into consideration. The term "Pilot-assisted CE (w/o noise)" in Figure 8 denotes the proposed pilot-assisted CE without the noise effect during the estimation process (only tracking errors due to channel time selectivity are taken into consideration).

It can be seen from the figure that the two-slot pilot-assisted CE scheme achieves a satisfactory performance while allocating only two slots for the proposed CE, which maintains a higher transmission data-rate in comparison with four-slot pilot-assisted CE schemes. The BER performance of the proposed channel estimator for broadband ANC degrades in comparison with the perfect CSI case; for BER $= 10^{-3}$ the $E_b/N_0$ degradation is about 5, 4, 4.5, and 7 dB when $N_b = 3$, 15, 47, and 79, respectively. This performance degradation is due to three factors: (*i*) the CE errors, (*ii*) the tracking errors, and (*iii*) imperfect self-information removal due to CE errors. In the case of CE without noise (long-dotted lines in Figure 8), where only the propagation errors due to the channel time selectivity are considered, the $E_b/N_0$ degradation, for BER $= 10^{-3}$, is about 3.5, 3.7, 3.8, and 4 when $N_b = 3$, 15, 47, and 79, respectively. The figure shows that the BER performance with proposed CE scheme, irrespective of $N_b$, is the same for $E_b/N_0 < 25$ dB since the performance improvement is limited by the CE errors and the tracking errors.

*5.3. Impact of Channel Time-Selectivity.* The impact of $f_D T_s$ on the BER performance with proposed CE scheme is discussed below. As $f_D T_s$ increases, the tracking ability against the channel fading variations tends to be lost. Figure 9 illustrates the BER performance as a function of $f_D T_s$ for $E_b/N_0 = 15$ dB, 30 dB, and 40 dB with $N_b$ as a parameter.

It can be seen from the figure that for $f_D T_s = 10^{-5}$ (which corresponds to about 2 km/h mobile terminal speed) almost the same BER performance is achieved irrespective of $N_b$. In the case of $f_D T_s = 10^{-4}$ (which corresponds to about 19 km/h mobile terminal speed), the BER performance slightly degrades irrespective of $N_b$ and $E_b/N_0$. On the other hand, as $f_D T_s$ increases to $10^{-3}$, which corresponds to about 190 km/h mobile terminal speed, the BER performance with $N_b = 16$ severely degrades since the tracking ability of the channel estimator against the channel time selectivity is lost.

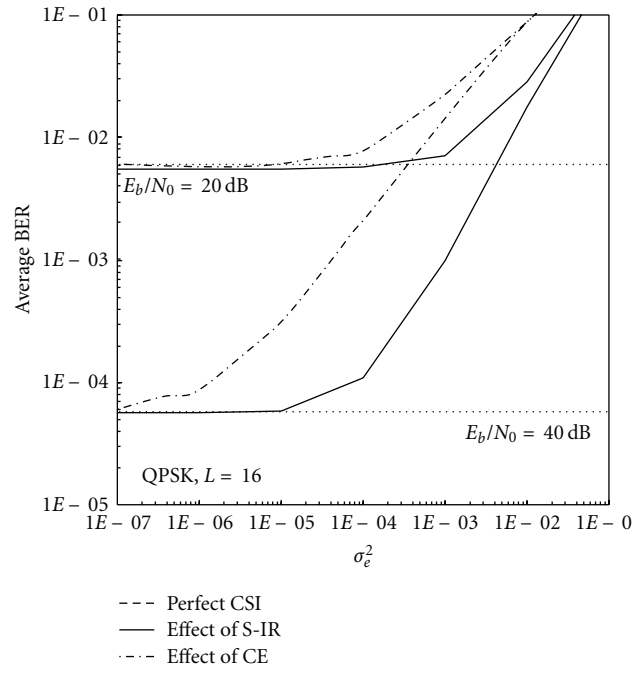


Figure 7: Effect of channel estimation error $\sigma_e^2$.

## 6. Conclusion

In this paper, we theoretically analyzed the performance of bidirectional broadband ANC communication based on OFDM radio access in terms of the channel estimator's MSE and BER. Assuming perfect timing and frequency synchronization, the achievable BER performance and the channel estimator's MSE for broadband ANC were evaluated by Monte-Carlo numerical and computer simulation. We discussed how much imperfect knowledge of CSI affects the BER performance of broadband ANC. Our results show that the BER performance of broadband ANC with practical CE gives a satisfactory performance for a low and

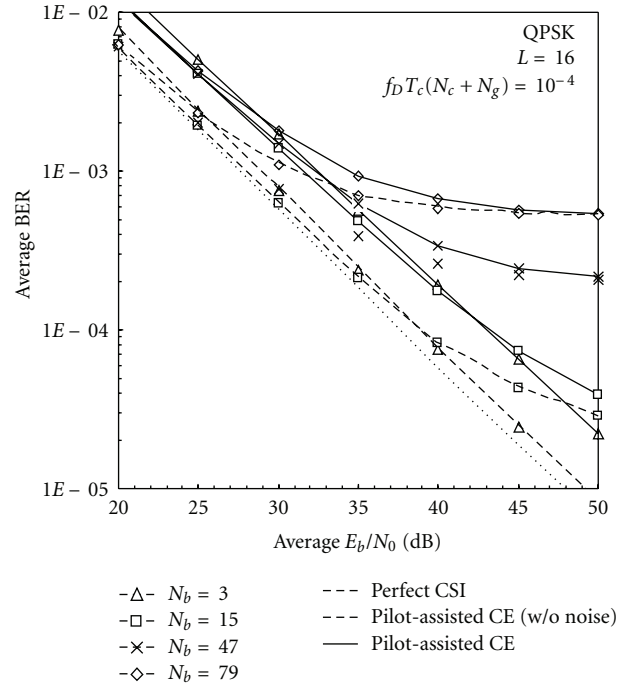


Figure 8: BER performance.

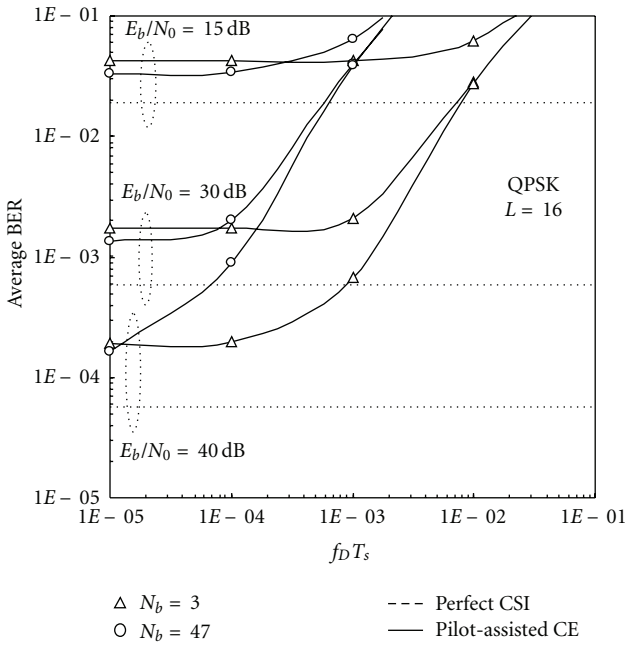


Figure 9: Impact of $f_D T_s$.

moderate mobile terminal speed in a frequency-selective fading channel.

The feedback of the estimated CSIs at the relay terminal was not considered in this paper. Time and frequency synchronization problems are a major design challenge for relay-assisted networks due to simultaneous signal reception from different users. Moreover, to provide bidirectional communication for more than two users either time division multiple access (TDMA), frequency division multiple access (FDMA), or code division multiple access (CDMA) can be used. These are left as an interesting future work. The performance analysis and comparison among digital network coding (i.e., PNC) and ANC with pilot-assisted CE are also left as an interesting future work.

## Appendices

## A. Interference Power of Desired Signal

The interference power of the desired signal due to imperfect knowledge of CSI is given by

$$\begin{aligned}\mathbf{P}_{j,\mathrm{II}} &= \mathbb{E}\left[\left|\left[\left(\mathbf{H}_j + \mathbf{E}_j\right)^{-1}\mathbf{E}_j\mathbf{d}_{\overline{j}}\right]_i\right|^2\right] \\ &= \mathbb{E}\left[\left[\left(\mathbf{H}_j + \mathbf{E}_j\right)^{-1}\mathbf{E}_j\mathbf{d}_{\overline{j}}\mathbf{d}_{\overline{j}}^H\mathbf{E}_j^H\left(\mathbf{H}_j + \mathbf{E}_j\right)^{-1H}\right]_{ii}\right].\end{aligned} \tag{A.1}$$

Applying the Sherman-Morisson formula [19], from (A.1) we obtain

$$\begin{aligned}\mathbf{P}_{j,\mathrm{II}} = \frac{E_s}{T_c}\,\mathrm{diag}\Bigg\{&\mathbb{E}\left[\left|\frac{E_j(0)}{H_j(0)+E_j(0)}\right|^2\right], \\ &\mathbb{E}\left[\left|\frac{E_j(1)}{H_j(1)+E_j(1)}\right|^2\right],\ldots, \\ &\mathbb{E}\left[\left|\frac{E_j(N_c-1)}{H_j(N_c-1)+E_j(N_c-1)}\right|^2\right]\Bigg\}.\end{aligned} \tag{A.2}$$

If we assume that the signal power is much larger than the channel estimation error variance (i.e., $\sigma_s^2 \gg \sigma_e^2$), we can expand $\Gamma(i) = \mathbb{E}[|E_j(i)/(H_j(i)+E_j(i))|^2]$ into a polynomial sum (i.e., $(1/(1+x)) = 1 - x + x^2 - x^3 + \cdots$) given by

$$\begin{aligned}\Gamma(i) = \mathbb{E}&\left[\left|\frac{E_j(i)}{H_j(i)}\right|^2\right] \\ &\times\left\{1 - 2\mathbb{E}\left[\left|\frac{E_j(i)}{H_j(\mathrm{i})}\right|^2\right] + 3\mathbb{E}\left[\left|\frac{E_j(i)}{H_j(i)}\right|^2\right]\right. \\ &\left.-4\mathbb{E}\left[\left|\frac{E_j(i)}{H_j(i)}\right|^3\right] + 5\mathbb{E}\left[\left|\frac{E_j(i)}{H_j(i)}\right|^4\right] - \cdots\right\}.\end{aligned} \tag{A.3}$$

We assume that $E_j(i)$ is a zero-mean Gaussian random variable, and, hence, it can be easily shown that the odd moments of (A.3) reduce to zero. Thus, (A.3) simplifies as

$$\begin{aligned}\Gamma(i) = \mathbb{E}&\left[\left|\frac{E_j(i)}{H_j(i)}\right|^2\right] \\ &\times\left\{1 + 3\mathbb{E}\left[\left|\frac{E_j(i)}{H_j(i)}\right|^2\right] + 5\mathbb{E}\left[\left|\frac{E_j(i)}{H_j(i)}\right|^4\right] + \cdots\right\}\end{aligned} \tag{A.4}$$

With reasonable small error, we can truncate the series in (A.4) only to its first two terms, and, then, the approximated expression for $\Gamma(i)$ is given by

$$\Gamma(i) \approx \frac{2\sigma_e^2}{\left|H_j(i)\right|^2}\left[1+3\frac{2\sigma_e^2}{\left|H_j(i)\right|^2}+5\left(\frac{2\sigma_e^2}{|H_j(i)|^2}\right)^2\right]. \quad \text{(A.5)}$$

Finally, combining (A.2) and (A.5), we obtain (23).

## B. Interference Power due to Imperfect Self-Information Removal

Interference power due to imperfect self-information removal resulting from imperfect knowledge of CSI is given by

$$\begin{aligned}\mathbf{P}_{j,\mathrm{III}} &= \mathbb{E}\left[\left|\left[\left(\mathbf{I}_{N_c}-\left(\mathbf{H}_j+\mathbf{E}_j\right)^{-1}\mathbf{E}_j\right)\mathbf{E}_{\overline{j}}\mathbf{d}_j\right]_i\right|^2\right]\\ &= \mathbb{E}\left[\left[\left(\mathbf{I}_{N_c}-\left(\mathbf{H}_j+\mathbf{E}_j\right)^{-1}\mathbf{E}_j\right)\mathbf{E}_{\overline{j}}\mathbf{d}_j\right.\right.\\ &\qquad\left.\left.\times\mathbf{d}_j^H\mathbf{E}_{\overline{j}}^H\left(\mathbf{I}_{N_c}-\left(\mathbf{H}_j+\mathbf{E}_j\right)^{-1}\mathbf{E}_j\right)^H\right]_{ii}\right].\end{aligned} \quad \text{(B.1)}$$

After some manipulations using the Sherman-Morisson formula [19], we obtain

$$\begin{aligned}&\mathbf{P}_{j,\mathrm{III}}\\ &= \frac{E_s}{T_c}2\sigma_e^2\mathbf{I}_{N_c}+\frac{E_s}{T_c}\,\mathrm{diag}\left\{\mathbb{E}\left[\left|\frac{E_j(0)}{H_j(0)+E_j(0)}\right|^2\left|E_{\overline{j}}(0)\right|^2\right],\right.\\ &\qquad\mathbb{E}\left[\left|\frac{E_j(1)}{H_j(1)+E_j(1)}\right|^2\left|E_{\overline{j}}(1)\right|^2\right],\ldots,\\ &\qquad\mathbb{E}\left[\left|\frac{E_j(N_c-1)}{H_j(N_c-1)+E_j(N_c-1)}\right|^2\right]\\ &\qquad\left.\times\left|E_{\overline{j}}(N_c-1)\right|^2\right\}.\end{aligned} \quad \text{(B.2)}$$

Using the same procedure as in Appendix A, we expand $\Upsilon(i)=\mathbb{E}[|E_j(i)/(H_j(i)+E_j(i))|^2|E_{\overline{j}}(i)|^2]$ into a polynomial sum and consider only the first two terms. Thus, $\Upsilon(i)$ is given by

$$\Upsilon(i) \approx 2\sigma_e^2\Gamma(i). \quad \text{(B.3)}$$

Finally, combining (B.1) and (B.3), we obtain (25).

## C. Noise Power

The total noise power for broadband ANC scheme with imperfect knowledge of CSI can be obtained as

$$\begin{aligned}\mathbf{P}_{j,\mathrm{IV}} &= \mathbb{E}\left[\left|\left[\left(\mathbf{H}_j+\mathbf{E}_j\right)^{-1}\left(\mathbf{H}_{1,j}\mathbf{n}_r+\mathbf{n}_j\right)\right]_i\right|^2\right]\\ &= \mathbb{E}\left[\left[\left(\mathbf{H}_j+\mathbf{E}_j\right)^{-1}\left(\mathbf{H}_{1,j}\mathbf{n}_r+\mathbf{n}_j\right)\right.\right.\\ &\qquad\left.\left.\times\left(\mathbf{H}_{1,j}\mathbf{n}_r+\mathbf{n}_j\right)^H\left(\mathbf{H}_j+\mathbf{E}_j\right)^{-1H}\right]_{ii}\right].\end{aligned} \quad \text{(C.1)}$$

Using the Sherman-Morisson formula [19], (C.1) can be written as

$$\begin{aligned}&\mathbf{P}_{j,\mathrm{IV}}\\ &= \frac{N_0}{T_c}\,\mathrm{diag}\left[\left|H_{1,j}(0)\right|^2,\left|H_{1,j}(1)\right|^2,\ldots,\left|H_{1,j}(N_c-1)\right|^2\right]\\ &\quad+\frac{N_0}{T_c}\,\mathrm{diag}\left\{\left|\frac{H_{1,j}(0)}{H_j(0)}\right|^2\mathbb{E}\left[\left|\frac{E_j(0)}{H_j(0)+E_j(0)}\right|^2\right],\right.\\ &\qquad\left|\frac{H_{1,j}(1)}{H_j(1)}\right|^2\mathbb{E}\left[\left|\frac{E_j(1)}{H_j(1)+E_j(1)}\right|^2\right],\ldots,\\ &\qquad\left.\left|\frac{H_{1,j}(N_c-1)}{H_j(N_c-1)}\right|^2\mathbb{E}\left[\left|\frac{E_j(N_c-1)}{H_j(N_c-1)+E_j(N_c-1)}\right|^2\right]\right\}\\ &\quad+\frac{N_0}{T_c}\,\mathrm{diag}\left[\frac{1}{\left|H_j(0)\right|^2},\frac{1}{\left|H_j(1)\right|^2},\ldots,\frac{1}{\left|H_j(N_c-1)\right|^2}\right]\\ &\quad+\frac{N_0}{T_c}\,\mathrm{diag}\left\{\left|\frac{1}{H_j(0)}\right|^2\mathbb{E}\left[\left|\frac{E_j(0)}{H_j(0)+E_j(0)}\right|^2\right],\left|\frac{1}{H_j(1)}\right|^2\right.\\ &\qquad\times\mathbb{E}\left[\left|\frac{E_j(1)}{H_j(1)+E_j(1)}\right|^2\right],\ldots,\left|\frac{1}{H_j(N_c-1)}\right|^2\\ &\qquad\left.\times\mathbb{E}\left[\left|\frac{E_j(N_c-1)}{H_j(N_c-1)+E_j(N_c-1)}\right|^2\right]\right\}.\end{aligned} \quad \text{(C.2)}$$

By expanding the $\mathbb{E}[|E_j(i)/(H_j(i)+E_j(i))|^2]$ into polynomial sum and taking the expectation of its individual terms, we obtain (26).

## Acknowledgment

This paper was supported, in part, by 2010 KDDI Foundation Research Grant Program.

## References

[1] R. W. Yeung, "Multilevel diversity coding with distortion," *IEEE Transactions on Information Theory*, vol. 41, no. 2, pp. 412–422, 1995.

[2] R. Ahlswede, N. Cai, S. Y. R. Li, and R. W. Yeung, "Network information flow," *IEEE Transactions on Information Theory*, vol. 46, no. 4, pp. 1204–1216, 2000.

[3] S. Y. R. Li, R. W. Yeung, and N. Cai, "Linear network coding," *IEEE Transactions on Information Theory*, vol. 49, no. 2, pp. 371–381, 2003.

[4] S. Zhang, S. C. Liew, and P. P. Lam, "Hot topic: physical-layer network coding," in *Proceedings of the 12th Annual International Conference on Mobile Computing and Networking (MOBICOM '06)*, pp. 358–365, Los Angeles, Calif, USA, September 2006.

[5] P. Popovski and H. Yomo, "Wireless network coding by amplify-and-forward for bi-directional traffic flows," *IEEE Communications Letters*, vol. 11, no. 1, pp. 16–18, 2007.

[6] S. Katti, S. S. Gollakota, and D. Katabi, "Embracing wireless interference: analog network coding," Tech. Rep., MIT Press, Cambridge, Mass, USA, February 2007.

[7] H. Gacanin and F. Adachi, "Broadband analog network coding," *IEEE Transactions on Wireless Communications*, vol. 9, no. 5, pp. 1577–1583, 2010.

[8] I. Marić, A. Goldsmith, and M. Médard, "Information-theoretic relaying for multicast in wireless networks," in *Proceedings of the IEEE Military Communications Conference (MILCOM '07)*, Orlando, Fla, USA, October 2007.

[9] Y. E. Sagduyu, D. Guo, and R. Berry, "On the delay and throughput of digital and analog network coding for wireless broadcast," in *Proceedings of the 42nd Annual Conference on Information Sciences and Systems (CISS '08)*, pp. 534–539, Princeton, NJ, USA, March 2008.

[10] K. Narayanan, M. P. Wilson, and A. Sprintson, "Joint physical layer coding and network coding for bi-directional relaying," in *Proceedings of the Allerton Conference on Communication, Control, and Computing*, Chicago, Illinois, USA, September 2007.

[11] M. Riemensberger, Y. E. Sagduyu, M. L. Honig, and W. Utschick, "Comparison of analog and digital relay methods with network coding for wireless multicast," in *Proceedings of the IEEE International Conference on Communications (ICC '09)*, Dresden, Germany, June 2009.

[12] Y. Hao, D. Goeckel, Z. Ding, D. Towsley, and K. K. Leung, "Achievable rates for network coding on the exchange channel," in *Proceedingsof the IEEE Military Communications Conference (MILCOM '07)*, Orlando, Fla, USA, October 2007.

[13] E. S. Lo and K. B. Letaief, "Network coding versus superposition coding for two-way wireless communication," in *Proceedings of the IEEE Wireless Communications and Networking Conference (WCNC '09)*, Budapest, Hungary, April 2009.

[14] F. Gao, R. Zhang, and Y.-C. Liang, "On channel estimation for amplify-and-forward two-way relay networks," in *Proceedings of the IEEE Global Telecommunications Conference (GLOBECOM '08)*, pp. 3670–3674, New Orleans, La, USA, December 2008.

[15] B. Jiang, F. Gao, X. Gao, and A. Nallanathan, "Channel estimation and training design for two-way relay networks with power allocation," *IEEE Transactions on Wireless Communications*, vol. 9, no. 6, pp. 2022–2032, 2010.

[16] F. Roemer and M. Haardt, "Tensor-based channel estimation and iterative refinements for two-way relaying with multiple antennas and spatial reuse," *IEEE Transactions on Signal Processing*, vol. 58, no. 11, pp. 5720–5735, 2010.

[17] T. Sjodin, H. Gacanin, and F. Adachi, "Two-slot channel estimation for analog network coding based on OFDM in a frequency-selective fading channel," in *Proceedings of the IEEE 71th Vehicular Technology Conference (VTC '10)*, Taipei, Taiwan, May 2010.

[18] Y. Li, J. H. Winters, and N. R. Sollenberger, "Simplified channel estimation for OFDM systems with multiple transmit antennas," *IEEE Transactions on Wireless Communications*, vol. 1, no. 1, pp. 67–75, 2002.

[19] C. D. Meyer, *Matrix Analysis & Applied Linear Algebra*, Society forIndustrial and Applied Mathematics, 2001.

[20] S. Coleri, M. Ergen, A. Puri, and A. Bahai, "Channel estimation techniques based on pilot arrangement in OFDM systems," *IEEE Transactions on Broadcasting*, vol. 48, no. 3, pp. 223–229, 2002.

[21] A. S. Lalos, A. A. Rontogiannis, and K. Berberidis, "Channel estimation techniques in amplify and forward relay networks," in *Proceedings of the IEEE Workshop on Signal Processing Advances in Wireless Communications (SPAWC '08)*, pp. 446–450, Recife, Brazil, July 2008.

[22] J. G. Proakis and D. K. Manolakis, *Digital Signal Processing*, Prentice Hall, Upper Saddle River, NJ, USA, 4th edition, 2006.

[23] D. C. Chu, "Polyphase codes with good periodic correlation properties," *IEEE Transactions on Information Theory*, vol. 18, no. 4, pp. 531–532, 1972.